Single-cell phenotypic characteristics of tolerance under recurring antibiotic exposure in *Escherichia coli*.

Silvia Kollerová[1], Lionel Jouvet[1], Julia Smelková [1], Sara Zunk-Parras[2], Alexandro Rodríguez-Rojas[2], Ulrich K. Steiner[1,2*]

[1]Department of Biology, University of Southern Denmark, Odense, Denmark

[2]Biological Institute, Freie Universität Berlin, Berlin, Germany

[*]Corresponding author

Email: ulrich.steiner@fu-berlin.de

Keywords: single-cell, microfluidics, evolution, antibiotic resistance, β-lactam, growth, survival, metabolism, persister, tolerance

Short title: Phenotypic characteristics of antibiotic tolerant cells

Abstract:

Non-heritable drug resistance, such as tolerance and persistence towards antibiotics, is little characterized compared to genetic resistance. Tolerance and persistence allow cells to survive application of antibiotics that are bactericidal to non-tolerant cells. Non-heritable drug resistance challenges antibiotic treatment, particularly of recurrent infections, and have implications towards heritable resistance evolution. Tolerant cells have commonly been characterized as growth arrested cells prior and during antibiotic application that quickly resume growth post-application. Here, we

explore characteristic of tolerant and susceptible *E. coli* single bacteria cells to different levels of recurrent antibiotic exposure and quantify their occurrence. In using a high throughput single-cell microfluidic device, we find that tolerant cells reduce their growth rate by about 50%, but contrary to previous findings do not go into growth arrest or near growth arrest. The growth reduction is induced by antibiotic exposure and not caused by a stochastic switch or predetermined state as previously described. Cells exhibiting constant intermediate growth survived best under antibiotic exposure and selection did not primarily act on fast growing cells, as expected for a β-lactam antibiotic. Control experiments on population cultures confirmed and challenged scaling of single cell findings to population level processes. Our findings suggest a prevalent type of tolerance that differs from previously described tolerance and persister characteristics. Our described characteristics and its high frequency of occurrence supports acclaims of an underappreciated role of tolerant cells towards resistance evolution.

Author Summary

Resistance to antibiotics is a major cause of treatment failure in modern medicine. In addition to genetic resistance, bacterial cells can sustain periods of bactericidal application in a so-called tolerant state. Previously tolerant cells were characterized by growth arrest prior and during exposure to antibiotics. Here, we show a distinctive type of tolerance that arises out of normally growing cells, where during antibiotic exposure, cell growth is slowed but does not go into growth arrest. Cells with an intermediate growth have the best survival, which is contrary to the assumptions of exposure to a β-lactam antibiotic where selection is assumed to act against the fastest growing cells and the least against non-growing cells. The novel characteristics of tolerance that we have uncovered provides bacteria with another route to evade antibiotics and that could be a considerable threat to the efficiency of antibiotic treatment.

Introduction

Resistance to antibiotics, in combination with slow progress in discovering novel antibiotics, poses a major challenge to modern medicine [1]. Antibiotic resistant cells sustain bactericidal concentrations of antibiotics through heritable genetically fixed mutations. In contrast, persistent and tolerant cells are in a non-heritable drug resistant phenotypic state. This state allows them to survive periods of bactericidal concentration of antibiotics by non- or very slowly growing[2–5]. They primarily arise from a non- or very slowly-growing sub-population of a susceptible population prior to antibiotic exposure [2–5]. The persister cell stage can be environmentally induced or stochastically switched to, hence, cells can dynamically alter states, and progeny of persiter cells are as susceptible as the parental population from which they derived [4,6]. Quantitatively, below 0.1% of cells in wild-type susceptible populations are persister cells.

Tolerant cells are more common than persister cells and they can also tolerate antibiotic exposures, and are also non- or very slow growing under antibiotic exposure [2]. Though compared to persister cells, tolerant cells can only sustain shorter durations of antibiotic exposure [4]. Under antibiotic application, tolerant cell populations show prolonged minimum duration of killing (MDK) without a change in the minimum inhibitory concentration (MIC), that is, they die slowly under antibiotic application even when exposed to very high concentrations.

A third class of cells that can sustain bactericidal concentration of antibiotics are viable but non-culturable cells (VBNC). In contrast to persister and tolerant cells, VBNC cells do not regain growth 3-4 hours post-antibiotic exposure, but instead remain at low metabolic activity in a deeper dormancy state and do not easily resuscitate, potentially due to a lack of intracellular ATP [7]. Persister and tolerant cells are therefore more susceptible to recurring exposure to antibiotics compared to VBNC cells [7]. VBNC cells are further phenotypically characterized by being small (2.3 ± 0.2µm for E. *coli*) and less elongated compared to persister cells [8].

70 The definition of these different cell types is not always consistent, and it can be difficult to distinguish
71 among them empirically, in particular when single-cell data is not available [3,4,9,10]. Only few studies
72 on resistance, tolerance, and persistence work at the single-cell level, and most of these few studies
73 evaluated persistence. Overall, these single-cell level studies highlight that that persister cells show
74 limited growth when exposed to β-lactam or other antibiotics that inhibit cell wall formation or cell
75 division [10–12], and that switching to persister stages can be irreversible or a reversible dynamic
76 stochastic process [12]. The stochastic switch to the rare persister state has been observed for growth-
77 limited cells within exponentially growing *E. coli* populations, with ~80% of persisters arising from the
78 non-growing sub-population prior to treatment, while the remaining persister cells originated from
79 cells that were growing prior to treatment [13,14]. Even though some high-quality single-cell data
80 exists on phenotypic characteristics of tolerant and persister cells, the quantification of the fractions
81 of susceptible, non-genetic tolerant and resistant cells remains scarce—including quantitative
82 understanding of cell type specific mortality rates and an accurate quantitative evaluation of cell
83 growth and division response to antibiotic application. However, such insights would provide deeper
84 understanding about the evolutionary importance of non-heritable tolerant cells for the evolution of
85 heritable resistance and efficacy of antibiotic treatment, as high frequencies of non-heritable tolerant
86 cells provide evolutionary reservoirs and increase the probability of genetically fixed resistance
87 mutations to occur [15–21].

88 Here, we use a quantitative demographic and phenomenological approach to quantify the fraction of
89 cells in a tolerant stage among susceptible stage cells, investigate how tolerant cells differ in their
90 single-cell characteristics compared to susceptible cells, and study what triggers changes in their
91 phenotypes. The focus is on tolerant cells, as persister cells are too rare to include in such quantitative
92 comparison at the single-cell level. Starting with a susceptible clonal population of cells that we expose
93 to recurrent antibiotic treatment at different concentrations, we track each cell for their growth,
94 division, and survival in a microfluidic device called a mother machine [22–24]. By exposing cells to a
95 β-lactam, ampicillin, that corrupts cell wall synthesis, we expected quickly-growing cells to be heavily

96 selected against, leaving primarily slow-growing tolerant cells that also arose from slowest-growing
97 population of cells prior to antibiotic exposure[3]. Tolerant cells should not be sensitive to antibiotic
98 concentrations beyond the MIC [3]. Tolerant cells are expected to regain normal growth rates within
99 hours post-antibiotic treatment, and such tolerant cells are expected to be the dominating cell type,
100 compared to VBNC cells, that do not regain growth past antibiotic application. We expected few cells
101 to switch by environmental induction to tolerant stages, i.e. antibiotic induced switching, as we
102 expected tolerant stages to be mainly predetermined prior to antibiotic exposure. We also expected
103 rare stochastic switching. To evaluate how our findings at the single-cell level might scale to cell
104 culture dynamics, we exposed cell cultures to similar recurring exposures of antibiotics and counted
105 colony forming units (CFU) before and after each exposure to antibiotics. In addition, we performed
106 an experiment by measuring the optical density dynamics of constantly exposed cell cultures to the
107 same levels of antibiotics.

108 RESULTS

109 **Mortality and selection for tolerance**

110 To select for and quantify characteristics of antibiotic tolerant cells, we exposed single-cells in a first
111 set of experiments to recurring antibiotic exposure of one of eight different concentrations. As
112 expected, the probability of cell death, i.e., the force of mortality, increased after the first exposure of
113 the susceptible parental population to the antibiotic, when exposed to MIC or higher concentrations
114 (Fig. 1b, Movie SI). Selection for tolerant cells was strong with about two thirds to three quarter of
115 cells dying before the second exposure period, when exposed to MIC or higher concentrations (Fig.
116 1a, Movie SI). Mortality peaked 30 to 60 minutes after the first 90-minute antibiotic exposure period,
117 which suggests that the force of selection peaked with a lag time of 2 to 2.5 hours after the start of
118 the first exposure. Survival patterns were similar at or above the MIC of 4 µg/ml (Fig. 1a, Cox
119 proportional hazard model Likelihood ratio test 477.1, $p<0.0001$, $n= 3496$; for post hoc testing see SI
120 Table S1). Neither of the two subsequent 90-minute exposure periods triggered a mortality force that

121 was as high as the first exposure period. After the initial rise in mortality triggered by the antibiotic
122 exposure, the probability of death declined, and increased again towards the end of the second
123 exposure period, though in a less synchronized way among cells exposed to different antibiotic
124 concentrations. The second peak force of mortality was reached about 30 to 90 minutes after the
125 second antibiotic exposure, resulting in a similar lag time to the first exposure, i.e., 2 to 3 hours.
126 Mortality rates continued to decline after the second peak of force of selection and fluctuated for the
127 remainder of the experiment. Note, cell numbers became small (~20-30 cells per concentration) and
128 estimates of mortality rates less reliable towards the end of the experiment.

129

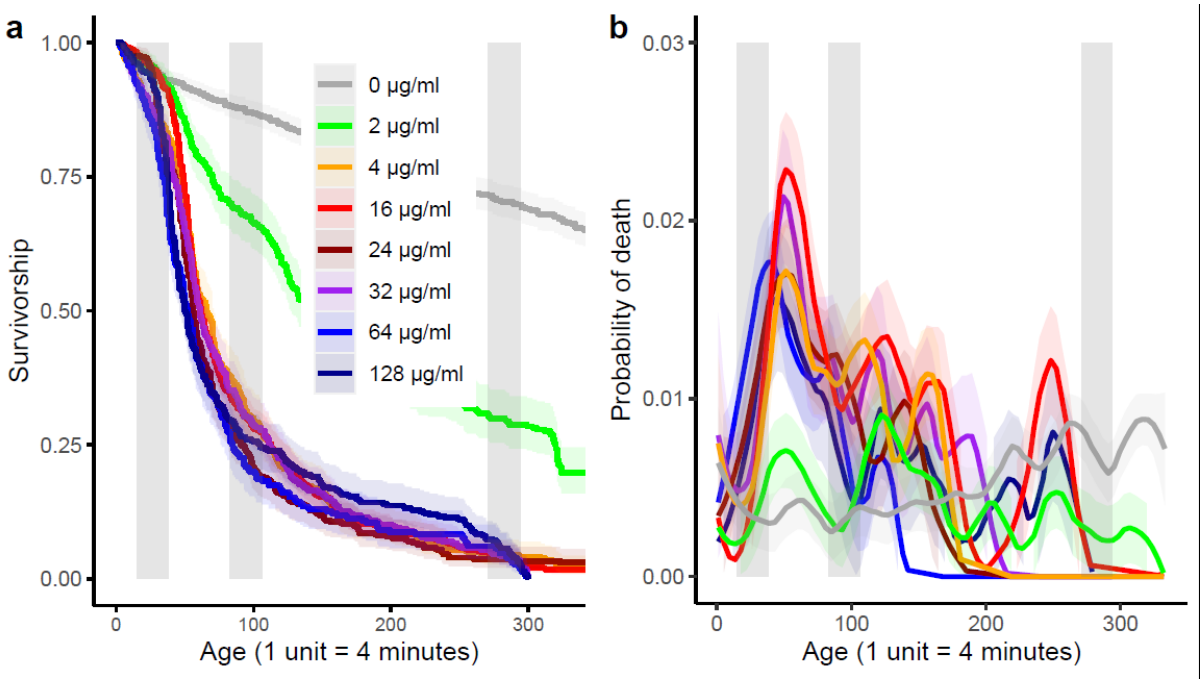

130

131 *Fig. 1: Survivorship curves (a) and probability of death, i.e., force of mortality (b) of cells exposed to*
132 *different levels of antibiotics across the duration of the experiment. The grey curves are control group*
133 *cells that were not exposed to any antibiotics. The grey vertical bars mark the exposure period to the*
134 *antibiotic. Kaplan-Meier survivorship curves (a) are shown with 95% CI. Probability of death curves (b)*
135 *are loess smoothed with 95% CI. X-axis units are given per 4 minutes to reflect the life imaging*
136 *frequency.*

137 **Division rate, size, and growth responses**

138 In contrast to the control group, cells that had been exposed to MIC or higher antibiotic concentrations
139 halved their division rate after the first exposure period, changing from ~2 to ~1 division per hour (Fig.
140 2a, Table 1). This reduction in reproductive rate was reached around 5.5 hours after the onset of the
141 first exposure. The division rates remained almost constant after the second exposure for another 6
142 to 7 hours, and then dropped off towards the end of the experiment.

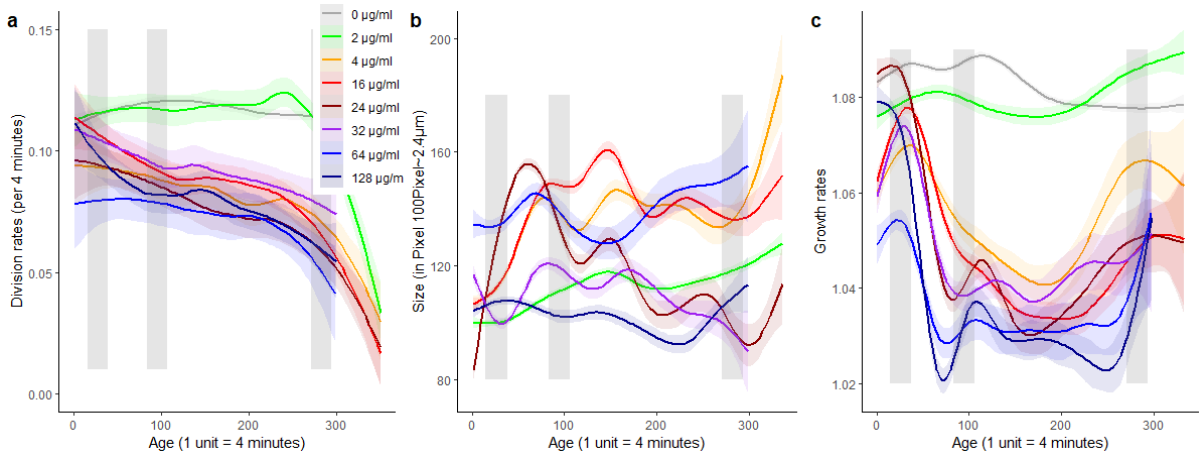

143

144 *Fig. 2: Cell division rates (a), cell size (in pixels with 100 pixels~2.4µm) (b), and growth rates (c) of cells*
145 *exposed to different levels of antibiotics across the duration of the experiment. The grey vertical bars*
146 *mark the exposure period to the antibiotics. Division rate (a) size (b) and growth rate (c) curves are*
147 *with 95% CI. Note, size data (b) for the control group (0µg/ml) was not available.*

148 Table 1: Model comparison among competing GAM models.

		DF	AIC
Division rate	**S(Age) + Concentr.**	**15.8**	**455232**
	S(Age)	8.4	487667
	Concentr.	8.0	455263
Size	**S(Age) + Concentr.**	**16.8**	**2455427**
	S(Age)	10.8	2460359

	Concentr.	8.0	2458502
Growth rate	**S(Age) + Concentr.**	**17.7**	**-1091065**
	S(Age)	10.5	-1073598
	Concentr.	9.0	-1087172

For each of the three response variables (Division rates, Size, and Growth rates), we compared three competing models. The best supported of these three models is highlighted in bold.

149

150 Average cell size remained approximately constant within a given antibiotic concentration. Although
151 we found a surprising amount of variation in size among cells exposed to different levels of antibiotics
152 (Fig. 2b, Table 1), there was no relationship between size and the levels of antibiotics. Cell growth
153 rates responded as predicted by declining during and after the first antibiotic exposure for cells
154 exposed to the MIC or above. We highlight here that growth rates only approximately halved (Fig. 2c,
155 Table 1), which starkly contrasts our predictions based on previous findings where persister or tolerant
156 cells were growth arrested or near growth arrested [4]. The induced growth reduction started about
157 30 minutes after the onset of antibiotic exposure, which is a lag time that corresponds to
158 approximately the doubling rate (division time) of the parental population. The lowered growth rates
159 stabilized about 4.5 hours after onset of the initial exposure period, suggesting substantial variance in
160 lag time among individual cells' growth response. Induced growth reductions depended partly on
161 antibiotic concentrations with higher levels of antibiotics leading to lower growth rates. However,
162 even with the highest antibiotic concentration, the growth rates did not drop below 1.02-1.03, i.e., 2-
163 3% cell elongation within 4 minutes. Further, after the second antibiotic exposure, growth did not
164 resume in the 11-hour phase without antibiotic application.

165 **Growth specific selection**

166 The growth rates as discussed above (Fig. 2c) are average growth rates at a given point in time, and
167 even though variance in growth rates does not increase substantially during the experiment (beyond
168 the expected increase due to decreasing number of cells towards the end of the experiment), selection
169 might still act preferentially against cells with high growth as expected from a β-lactam antibiotic and
170 as previously described for persister and tolerant cells [6]. To evaluate the possibility of such
171 differential selection based on cell growth we analysed together all cells exposed to MIC or above, and
172 then separated them out into three growth categories: cells that did not grow or shrank (growth
173 arrested cells with growth rates <1.0), cells that grew at low to intermediate rates (growth rates 1.0-
174 1.1), and cells that grew quickly (growth rates >1.1) (Fig. 3a). Note that cells can switch dynamically
175 among these categories throughout the experiment and that mortality and survival is associated only
176 with the current growth rate of a cell and not a cell's growth rate averaged across time. As expected,
177 quickly growing cells showed increased probabilities of death upon exposure to antibiotics, but
178 contrasting to our expectations, the probability of death of growth arrested cells increased
179 substantially upon exposure to antibiotics, whereas the probability of death of slow-intermediate
180 growing cells did not change (Fig. 3b, see also SI Table S2 and Table S3).

181 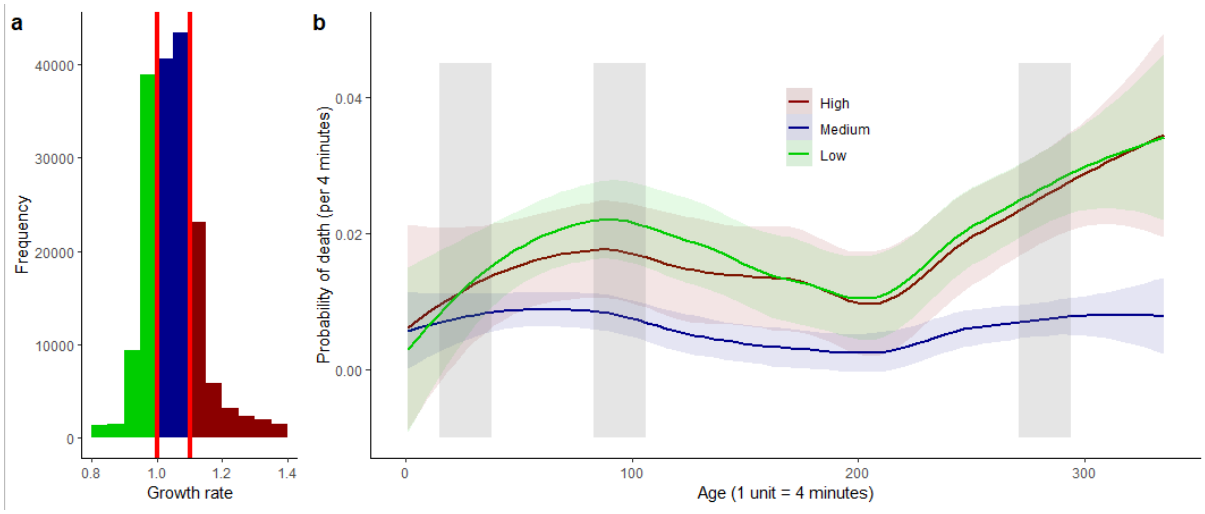

182 *Fig. 3: Cell growth rate distribution divided into three categories: growth arrested (shrinking or non-*
183 *growing; green), intermediate growth (blue), and fast growth (red) (a), and probability of death for*
184 *these three groups of growth arrested, intermediate, and quickly-growing cells across the duration of*

185 *the experiment (b). The grey vertical bars in panel (b) mark the exposure period to the antibiotics. Note*
186 *that cells can switch among growth categories throughout the experiment, that is cells are categorized*
187 *according to their current cell growth rate. For this analysis, we have combined cells across levels of*
188 *antibiotic exposure ≥4 µg/ml and excluded all cells exposed to 2 µg/ml. A statistical model comparison*
189 *showed that mortality differed substantially among the three growth category groups: ΔAIC 25.8*
190 *comparing a growth category model and a null model, see also Supplemental Information. Classical p-*
191 *value post-hoc analyses showed that quickly growing and growth arrested groups did not differ from*
192 *each other in age at death, but the intermediate group did.*

193 To verify the robustness of our finding that selective mortality is dependent on growth rates, and to
194 broaden our understanding of how growth influences beyond the current growth rate (Fig. 3b), we
195 did three comparisons between average growth rates of surviving to or dying before specific point in
196 time during the experiment. First, we compared the average growth rate (averaged across time) of
197 cells that survived the first exposure period to those that died before the first exposure period.
198 Second, we compared the average growth rate of cells dying during or shortly after the first exposure
199 period (cut off at peak of first mortality) to those surviving past the first peak of mortality, and third
200 we compared similarly for cells that died between the first peak of mortality and the second peak of
201 mortality to those that survived past the second peak of mortality (Table 2). Before the first exposure,
202 cells that died had lower average growth rates compared to those that survived past the first
203 exposure, showing that without selection of antibiotics slower growing cells are preferentially selected
204 against. Cells that died during the first exposure or shortly after, i.e., during times of strong selection,
205 had slightly higher growth rates than those that survived past this first increased selection period. This
206 pattern of growth dependent selection remained for the next period of increased selection after the
207 second antibiotic exposure. These findings support our initial prediction that faster growing cells
208 would be preferentially selected against under antibiotic exposure. However, note that the effect sizes
209 (growth differences) among surviving and dying cells are small, even though they are significantly

210 different. We interpret our findings on growth specific selection under antibiotic exposure as not
211 primarily acting on fast-growing cells.

212 Table 2: Differences in average growth rates of cells surviving past or dying during or after specific
213 points in time.

PERIOD	0 – 60 MIN	60 – 328 MIN	328 – 600 MIN	+600 MIN
GOWTH RATE OF CELLS DYING DURING PERIOD (±STDEV)	1.047 (±0.039)	1.067 (±0.032)	1.057 (±0.030)	1.045 (±0.027)
GROWTH RATE OF CELLS SURVIVING PERIOD (±STDEV)	1.072 (0.0412)	1.060 (±0.035)	1.050 (±0.028)	
AIC GROWTH DURING/AFTER	**-8020.8**	**-8816.3**	**-3170.8**	
AIC NULL MODEL	-7985.4	-8772.0	-3161.4	
ΔAIC	35.4	44.3	9.4	

214 *Model comparison among a null model (intercept only model) and a model with the two groups of cells*
215 *dying during a particular period or surviving that period as explanatory variable and the mean growth*
216 *rate (per 4 min) as response variable. Three sets of models were fit, one for each period [0 min – 60*
217 *min; 60 min – 328 min; 328 min – 600 min]. A Gaussian error structure was used to fit these models.*
218

219 **Robustness of growth rates within cells**

220 In Fig. 2c, we investigated the average growth rate at a given time point. As cells can dynamically alter
221 growth rates between the current and a future point in time, we correlated a cell's current growth
222 rate to its growth rate in the future. Overall correlation between an individual's cell growth rate at a
223 given time t and its growth rate in the immediate future (time *t*+1 [4 minutes later]) or future time
224 points (time *t*+3 [12 min later]; time *t*+5 [20 minutes later]) was weak (Fig.4, Table 3), that is a cell's
225 current growth rate does not well predict its future growth rate. However, there was the exception
226 for cells with intermediate growth rates (1.0-1.1), that showed a strong correlation between current
227 and future growth (Fig. 4), illustrating robust constant growth. Growth arrested cells (growth rate <1
228 at time t) tended to increase in their growth rates in the at future points in time, while quickly-growing

229 cells (growth rates >1.1 at time t) tended to decrease their growth rates (Fig. 4). Overall, intermediate
230 growing cells showed robust and stable growth rates as illustrated by them following tightly the direct
231 correlation line (Fig. 4), while growth arrested and quickly-growing cells deviate from this direct
232 correlation. Across cells, we observed substantial temporal dynamics in growth rates. Growth arrested
233 and quickly-growing cells seemed to be more affected by the concentration of antibiotics, which
234 suggests that the growth rate responses to different concentrations of antibiotics shown in Fig. 2c are
235 mainly influenced by the fastest growing and growth arrested cells.

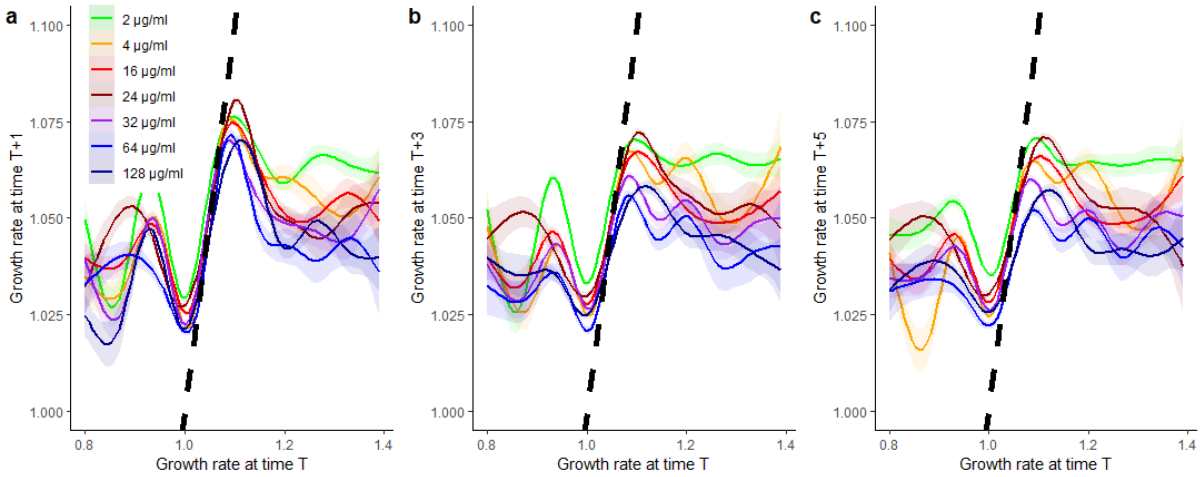

236 *Fig. 4: Correlation in cell growth rates at a given time t, compared to growth rates at time t+1 (4*
237 *minutes later) (a), t+3 (12 minutes later) (b), and t+5 (20 minutes later) separated out into populations*
238 *recurrently exposed to different levels of antibiotics (as described in the main experiment). All growth*
239 *rate correlations are fitted with a GAM with 95% CI. The dashed black line illustrates the direct*
240 *correlation among time points.*

241 Table 3: Model comparison among competing GAM models, for correlation of current growth rates to
242 growth rates at future points in time.

	MODEL	DF	AIC
GROWTH T+1	**Concentr. + S(Growth by Concentr)**	**70.3**	**-441151**
	Concentr. + S(Growth)	17.0	-440468

	S(Growth)	11.0	-438626
	Concentr.	8.0	-425891
GROWTH T+3	**Concentr. + S(Growth by Concentr)**	**69.2**	**-421883**
	Concentr. + S(Growth)	17.0	-421503
	S(Growth)	11.0	-420235
	Concentr.	8.0	-407188
GROWTH T+5	**Concentr. + S(Growth by Concentr)**	**69.0**	**-412563**
	Concentr. + S(Growth)	17.0	-412180
	S(Growth)	11.0	-410925
	Concentr.	8.0	-398709

Best supported model for each response variable (Growth t+1, t+3, t+5 respectively) is highlighted in bold. GAM models are fitted with the restricted maximum likelihood method, a smoothing parameter for Growth rate at time t with a shrinkage version of a cubic regression spline as smoothing parameter (bs=cs) and/or the concentration, including a model that accounts for the interaction of the two explanatory variables, growth rate and concentration of antibiotics. Growth rates are fitted with a Gaussian error structure and an inverse link function.

Population level responses

Much research investigating antibiotic tolerance and persistence has been done at the population level, which makes it challenging to understand mechanisms and describe characteristics operating at the single-cell level. At the same time, scaling single-cell characteristics to population level can be challenging, in the following section we therefore report on the control experiments done in cell cultures. For these cell culture experiments we took two approaches that were suitable as control experiments: CFUs were counted before and after each exposure period to antibiotics in order to

258 mimic the recurrent application of antibiotics as in the single-cell experiments, or we evaluated cell
259 densities (OD) under constant antibiotic concentrations to understand longer exposure to antibiotics.
260 Cell cultures exposed up to the MIC showed similar dynamics in terms of numbers of CFUs when
261 recurrently exposed to antibiotics (Fig. 5a). For higher levels of exposure, the higher the antibiotic
262 concentration the stronger the reduction in CFUs, and the stronger the increase after the first
263 exposure to antibiotics was relieved. The response to the second and third exposure and antibiotic
264 release was dampened, which aligns with predictions of selection for tolerant cells as revealed for the
265 single-cell findings. During the long recovery time after the second exposure, most cultures, except
266 those previously exposed to 64 and 128 µg/ml, reached densities that likely imposed growth limitation
267 due to resource limitation (i.e., the cultures approached stationary phase). The decline in CFU during
268 the recurrent exposure shows the continued susceptibility of the cells after series of selection due to
269 antibiotic exposure. When populations were permanently exposure to antibiotics (Fig. 5b), they, as
270 expected, initial increased in density before densities were reduced to very low levels for all cultures
271 exposed to MIC or above MIC concentrations, illustrating the susceptibility of the initial population.

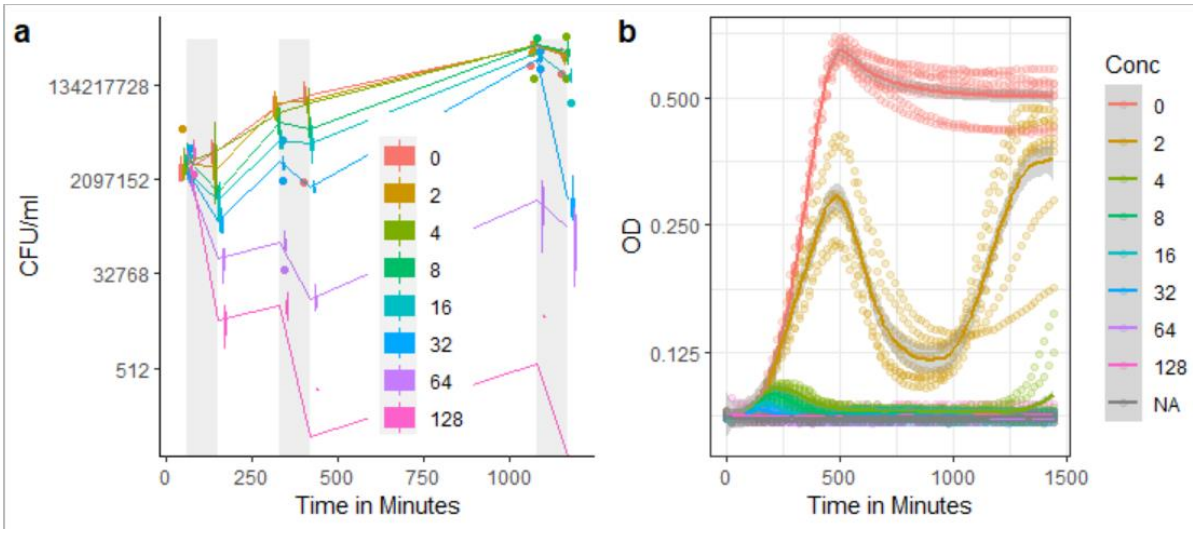

Fig. 5: Colony forming units (CFU) (a), and optical density, OD_{600} (b) of cell cultures exposed to different levels of antibiotics across the duration of the experiment (a) or constant exposure to antibiotics throughout the experiment (b). The grey vertical bars (a) mark the exposure period to the

antibiotics. CFU (a) are plotted as boxplots with line connecting mean number of CFU per time when CFU were counted. Single data points are outliers. Note, a jitter is added (a) for better visibility. For the OD curves (b) the dotted lines show the different replicates. NA in panel (b) is the negative control, i.e., no bacteria added to medium. CFU (a) and OD (b) are plotted on a log scale.

272

273 DISCUSSION

274 We report a previously undescribed, combination of phenological single-cell characteristics in *E. coli*
275 in response to recurring exposure to a β-lactam antibiotic. A substantial fraction (>25%) of cells
276 survived antibiotic exposure independent of the level of antibiotics (Fig. 1a, see also findings at cell
277 culture for <64 µg/ml; Fig. 5a), this is a considerably larger fraction than previously described for
278 persister cells (<0.1%) at similar concentrations [2–4]. In line with previous findings and as expected
279 the MIC marked a survival threshold, illustrating that the initial population was susceptible and not
280 resistant (Fig. 1), this susceptibility was also confirmed when evaluated at the cell culture level (Fig.
281 5). Our results show that the susceptible clonal parental population consists of phenotypically
282 heterogeneous cells, whereby the cells have different capacities to sustain exposure to antibiotics,
283 leaving predominantly tolerant cells after the first period of exposure.

284 We found reduced cell growth and division rates under antibiotic exposure, but this reduction was
285 quantitatively different compared to previously described tolerant cells. Growth reduction in our cells
286 was only halved, while other studies have reported growth arrest or near growth arrest of tolerant
287 and persister cells [2,4,10,11]. In contrast to previously described characteristics of tolerant and
288 persister cells, after release from antibiotics, we did not observe resumption of normal growth within
289 2-4 hours [3,4]. Such a lack of growth resumption is characteristic of some persister cells (type II) and
290 VBNC cells, however VBNC are found in complete growth arrest and are characterized by a small cell
291 size, and these specific persister (type II) cells are not environmentally induced but predetermined
292 [8,11], features not found in our study. Quantitative comparison to understand the resumed

293 population growth at the cell culture level (Fig. 5) in light of the single cell growth reduction (Fig. 2)
294 are challenging, as it remains opaque whether population growth dynamics are driven by increased
295 cell division rates, increased cell growth, or altered mortality rates [25]. In addition, with respect to
296 heterogeneous selection and cell size, the average cell size remained constant over the course of the
297 experiment (Fig. 2b) suggesting that selection did not favor small cells like VBNC cells, or increased cell
298 size as observed for increased frequencies in filamentation of cells. Filamentation in bacteria is the
299 continued cell elongation without dividing. Finally, variation in cell size did not increase substantially
300 across the course of the experiment, which would have been predicted had higher proportions of
301 small cells (VBNC) and filamentous cells simultaneously emerged.

302 Our observations differ from genetically fixed resistant cells in various ways. First, at the single-cell
303 level, unlike resistant cells, we did not find graded survival to different levels of antibiotics (Fig. 1 &
304 2a), although at the cell-culture level graded responses in CFUs were observed (Fig. 5). Second, our
305 cells halved their growth rates (50% reduction in cell elongation rates) under exposure (Fig. 2c),
306 whereas a 20% reduction in population growth (evaluated in cell cultures) is already considered to be
307 an extreme growth cost for resistant cells [26]. Third, in contrast to resistant cells, our cells showed
308 continued susceptibility to repeated exposure to antibiotics (Fig. 1, Fig. 5a). Finally, resistance is not
309 expected for our single-cell findings, as our population of cells was directly derived from a susceptible,
310 standard *E. coli* lab strain K-12 MG1655 (see also Fig. 5b). A heteroresistant population, i.e., one
311 composed of multiple sub-populations that differ in their genetically fixed resistance to antibiotics
312 (exemplified by different MIC), should have left, post exposure, a resistant population with graded
313 responses to increased levels of antibiotic concentrations. However these were patterns that we did
314 not find in survival, division or growth rates (Fig. 1&2) [26]. Despite the isogeneic origin, our initial
315 population was heterotolerant with a high fraction of cells (>25%) surviving the first exposure and
316 continued showing dampened sensitivities with respect to mortality for following exposure periods
317 (Fig. 2a). Such continued, but dampened, sensitivity could be explained by stochastic switching of

318 smaller fractions of cells out of the tolerant state, which might be related to stochastic gene expression
319 prior, during, and after exposure to antibiotics [27].

320 In contrast to previously described tolerant cells, our tolerant cells did not arise from stationary phase
321 cells, they were also not growth-arrested or slow growing prior to exposure [2,4,6,11]. These growth
322 characteristics have important implications for the evolution of resistance. "Classical" tolerant and
323 persister cells only contribute to resistance development through repeated rounds of population
324 expansion by their offspring, as they are growth arrested prior to and during antibiotic exposure,
325 whereas our tolerant cells contribute before, during, and after antibiotic exposure to population
326 expansion, and therefore provide continued opportunities for the accumulation of mutations towards
327 resistance [19]. Our tolerant cells cannot, *a priori*, be distinguished from non-tolerant cells by their
328 reduced growth rate [11]. Rare types of persister cells, that have previously described, did not arising
329 from stationary phase cells and showed slow growth resumption post-exposure, these cells were
330 almost growth arrested under antibiotic exposure [10], and we did not find such growth arrest for our
331 cells.

332 Our finding that intermediate growing cells that exhibited robust growth rates, had higher survival
333 rates compared to growth arrested, and quickly-growing cells (Fig. 3 & 4), is surprising to us as we had
334 predicted growth arrested cells to be the least affected by β-lactam exposure [2,4,6,11]. Our findings
335 might indicate that tolerant cells with high survival have more balanced and robust intrinsic
336 metabolism (homeostasis) and less dynamic biochemical changes, which contrasts with molecular
337 level findings that link tolerance to a perturbed biological network [15].

338 The tolerant state that our cells are characterized by is an induced state, and not an instantaneous
339 switch, a pre-existing state [4], or a rare occasional stochastic switch to a persistence or tolerant state
340 out of exponentially growing cells as previously described [11]. Similar induced switching as we find
341 has been found for fluoroquinolone-induced persistence [28] and aligns with findings where increased
342 tolerance and persistence were induced by antimicrobial peptide exposure [10,29]. The switch to the

343 induced tolerant state we observe takes on average 2 to 3 hours, with substantial among-cell
344 variation, emphasizing that it is not an instantaneous switch. This lag time spans a minimum of 2 to 3
345 divisions or a time during which the initial cell's biomass increases by about 4-8 times, and this lag
346 time is independent of the levels of antibiotic exposure. The emergence of our tolerant cells out of an
347 exponentially growing population suggests that the evolution, or at least the maintenance, of
348 tolerance is not conditional on nutrient limiting condition as has previously been suggested to be the
349 favorable evolutionary route [30].

350 Our finding that cells cannot be easily identified prior to antibiotic exposure by their reduced growth
351 rates also supports findings that there are various evolutionary routes to tolerance [4,5,15,31]. This
352 contrasts with our knowledge of the much better understood evolution of genetically fixed resistance,
353 which tends to arise from mutations in a few defined genes that relate directly to the mechanism by
354 which the antibiotic acts [15]. The diversity of evolutionary paths to tolerance is illustrated by
355 experimental evolution studies that evolved high tolerance by repeated exposure to ampicillin and
356 showed that tolerance was achieved through increased lag time [32]; other experimental evolution
357 studies, which exposed stationary phase cells, evolved tolerance without prolonged lag times [33],
358 and still other experimental evolution studies found again other mutations [15,34].

359 Our findings contrast in surprising ways with previous findings on tolerance and persistence. We
360 therefore need to ask why we find such differences. For instance characteristics and frequency of
361 persisters depend on culture conditions and growth phase, even when the same species, strains, and
362 antibiotics are used [45]. Studies that enriched persisters by preselecting dormant cells [14,46] could
363 not detect our cell types, as we did not find clearly predefined characteristics [10]. Results might also
364 be biased when working with high-frequency persister mutants, such as hip mutants, as they show
365 altered characteristics compared to wild type cells [11]. Growth medium can influence phenotypes,
366 such as the filamentation rate, or the recovery rate from filamentous states [22,24]. Exposure time to
367 antibiotics applies different selection pressure for tolerance, with our exposure time of 90 minutes

368 being shorter compared to other experiments that select cells by exposing them to ~5 hours [10,11].
369 The quantitative depth of our results, reporting on several hundred tolerant cells selected from a few
370 thousand cells, also differs from other studies. The exciting core findings of Goormaghtigh and Van
371 Melderen [10] rely on 23 persister cells selected out of more than 100,000 cells. In sum, the
372 characteristics we have described are unlikely to be explained solely by the experimental setup and
373 growth conditions and are more likely novel tolerance characteristics.

374 Future investigations should explore varying exposure time and varied inter exposure time periods.
375 Prolonged treatment cycles can cause tolerant strains to attain resistance at higher rates [16], while
376 multi-drug treatment can prolong time to tolerance evolution [47], another dimension that could
377 easily be explored in the future. Different strains can be explored, but such exploration should be
378 systematic, as part of the diverse findings on tolerance might be caused by small differences in
379 experimental settings not related to the main target [15]. A rigorous phenomenological exploration,
380 as we have done, can provide synergistic insights for tailored molecular exploration. Such molecular
381 exploration will be interesting as of the expected diversity of molecular and evolutionary paths to
382 tolerance. This molecular diversity likely results in a diversity of phenomenological characteristics of
383 tolerance. For instance, our cells did not show alterations in cell size, which suggests that our tolerance
384 might not be related to known tolerance mechanisms to β-lactams, where filamentation rate is
385 increased, which in turn stops ampicillin from efficiently targeting the cells [10,34,48]. Our approach
386 also illustrates the challenge and potential of scaling from single cell to the population level, a link that
387 will provide a deeper understanding of the evolutionary potential towards resistance, but which is still
388 rarely explored in detail. Our single-cell study is a cohort study and not a cross-cohort study like cell
389 culture experiments, however cross-cohort studies can be achieved at the single cell level. Other
390 differences, such as inter cellular communication, quorum sensing, nutrient limitation, or density
391 dependence, among single-cell and cell culture explorations are more challenging to circumvent but
392 these differences can reveal important conditions that help to reveal potential tolerance mechanisms.
393 Microfluidic systems prevent density dependent and nutrient limiting regulations, single-cell level

394 understanding affords a distinction among mortality, division, size, and growth effects, which are
395 surmised by the cell culture level measurements of CFU or OD. The diversity and partly contrasting
396 findings on persister and tolerant cells, illustrates that we are still on the verge of understanding the
397 role and mechanisms of tolerance, and standardized and comparative studies are needed to solidify
398 and advance our current understanding. Nevertheless, the importance of tolerance is reflected in our
399 cell culture experiments, where population crashes were prevented by tolerant cells when the
400 population was exposed recurrently to antibiotics. Our results support the idea of a novel form of
401 tolerance, where there is no pre-determined slow growth, no growth arrest, and no quick resumption
402 of growth. These characteristics have implications for the evolution of resistance in providing
403 evolutionary reservoirs and increased mutant supply; this novel combination of characteristics might
404 even call for a wider definition of what tolerant cells are. As for applied implications on medical
405 treatment, we need to be cautious about interpretation, because directly relating *in vitro* to *in vivo*
406 results for antibiotic treatment remains challenging.

407 MATERIALS AND METHODS

408 We conducted four experiments, three of them with three antibiotic exposure periods of 90 minutes,
409 two of these experiments collected single-cell data and one cell culture level data, i.e. CFU counts. The
410 fourth experiment, which was at the cell culture level, continuously exposed cells to antibiotics and
411 served as a control experiment. All experiments, single-celled and cell culture experiments, were done
412 in supplemented minimal media (M9), and all cultures were derived from *E. coli* strain MG1655, a K12
413 strain. We chose antibiotic concentrations similar to previously explored ranges, that spanning from
414 below MIC to >30 times MIC, and exposed cells to antibiotics for periods that would cover three to
415 four divisions under non-antibiotic conditions. Post-exposure recovery times were also chosen on
416 previous results reporting on regained growth of persister cells within 3-4 hours post-treatment [10–
417 12]. We choose ampicillin as antibiotic, a β-lactamase that inhibits bacterial cell wall synthesis,
418 because this antibiotic has been extensively used in previous persister studies [11]. Comparing growth

419 dynamics, size, division dynamics, and mortality in response to recurring exposure to antibiotics allows
420 us to differentiate among tolerant and VBNC cells, and in comparing lag times we differentiate
421 antibiotic induced and stochastic switching to tolerance.

422 For the experiments with recurrent exposure, the first exposure period was 60-150 minutes past onset
423 of the experiments, the second exposure period was 330-420 minutes past onset of the experiments,
424 i.e. 180 minutes past the first exposure period, and the last exposure period was 1080-1170 minutes
425 past onset of the experiments, i.e. 660 minutes past the second exposure period. For the single-cell
426 experiments concentrations of ampicillin during the exposure periods were set to 2, 4, 16, 24, 32, 64
427 or 128µg/ml. As comparison and reference, data from another experiment was added as control
428 group, where cells were never exposed to antibiotics [23]. For the experiments at the cell culture level,
429 the concentrations of 0, 2, 4, 8, 16, 32, 64 or 128µg/ml were used, and in addition a negative control
430 testing for potential contamination was done.

431 To collect phenological data at the single-cell level, each cell was tracked by time-lapse life-imaging
432 (15 frames/hour) in a microfluidic (PDMS) chip, a mother machine [23], that was placed under a
433 temperature-controlled (37°C) inverted microscope. The cells loaded into the microfluidic chip came
434 from an exponentially growing culture. Given that the cell culture the loaded cells originated from was
435 in exponential growth phase, the vast majority of cells loaded were in an exponential growth phase
436 [24]. The microfluidic chip the cells grew in contained four main laminar flow channels (feeding
437 channels) and hundreds of dead-end side channels, in the latter the rod-shaped bacteria-cells grew.
438 Only one focal cell, the one closest to the dead-end of the side channel, was tracked for its growth
439 (cell elongation), size, time of each division, and death. Cell death was determined by propidium iodide
440 (PI) that emits a strong fluorescent signal when the cell wall lysis—the moment the PI can enter the
441 cell—and bonds to the cells' DNA. Image analysis was performed using a customized software and the
442 resulting data was subsequently analysed in program R [49] using general linear, generalized linear,
443 and nonlinear (Generalized Additive Models, GAM) models. Models were compared based on

444 information criteria (AIC)[50]. Kaplan-Meier survivorship curves (Fig. 1a) are computed with the
445 survival package (survfit function), probability of death curves (Fig. 1b) are plotted with a loess
446 smoothing function (geometric_smooth function; package ggplot2). Competing GAM models (Table
447 1) are fitted with the restricted maximum likelihood method (REML), a smoothing parameter for age
448 with a shrinkage version of a cubic regression spline as smoothing parameter (bs=cs) and/or the
449 concentration. Division rates (Fig.2a) are fitted with a loess smoothing function (geometric_smooth;
450 package ggplot2) using a binomial error structure with a logit link function, size data (Fig. 2b) is fitted
451 with a GAM model applying a Gaussian error structure and an identity link function, and the Growth
452 rates (Fig. 2c) are fitted with GAM model using a Gamma error structure and an inverse link function.
453 Note, smoothing functions (GAM) are highly sensitive at the extremes as partly illustrated by the
454 diverse initial average cell sizes (Fig. 2b) of cells that came from the same parental population and that
455 had not yet been exposed to antibiotics during the 60-minute lasting acclimation phase. Probability of
456 death curves (Fig. 3b) are plotted with a loess smoothing function with 95% CI (geometric_smooth;
457 package ggplot2). More details on the microchip production, loading of the chip, the bacteria growth,
458 imaging, and analyses on the single-cell experiments are given in the supplemental material.

459 To collect the number of colony forming unit (CFU) data and the cell culture density data (OD_{600}), we
460 initially seeded these experiments using cells from an exponential growing culture. Each experiment
461 had 8 replicates, the experiments were done in 96 well-plates, and cells grew at 37°C and vigorous
462 shaking in their respective well (see Fig. S1 for details). To achieve the sequence of antibiotic exposure,
463 the cell culture plates were centrifuged, super-natant was discarded and cells were resuspended in
464 fresh media with or without antibiotics depending on treatment. The concentration changed to match
465 those used for the single-celled experiments and CFU were counted by serial dilution plating on LB
466 agar plates when antibiotic exposure changed. To track cell culture density at constant antibiotic
467 exposure, the initial 8 replicates for each concentration of the antibiotic exposure were incubated at
468 37°C and shaking in a 96-well-plate and the optical density (OD600) was measured every 20 minutes
469 for 24 h in a plate reader Synergy H1 (Biotek, Germany). Fig. 5b the OD curves are fitted with a loess

470 smoothing function with 95% CI (geometric_smooth with a span of 0.1; package ggplot2). Further
471 information on these cell culture experiments is given in the supplemental material.

472 Acknowledgements
473 We thank Jens Rolff and Sophie Armitage for comments and discussions.

474

475 References

476 1. Ventola CL. The antibiotic resistance crisis: causes and threats. P T J. 2015;40: 277–83.
477 doi:Article

478 2. Brauner A, Fridman O, Gefen O, Balaban NQ. Distinguishing between resistance, tolerance
479 and persistence to antibiotic treatment. Nature Reviews Microbiology. Nature Publishing
480 Group; 2016. pp. 320–330. doi:10.1038/nrmicro.2016.34

481 3. Brauner A, Shoresh N, Fridman O, Balaban NQ. An Experimental Framework for Quantifying
482 Bacterial Tolerance. Biophys J. 2017;112: 2664–2671. doi:10.1016/J.BPJ.2017.05.014

483 4. Balaban NQ, Helaine S, Lewis K, Ackermann M, Aldridge B, Andersson DI, et al. Definitions
484 and guidelines for research on antibiotic persistence. Nat Rev Microbiol. 2019;17: 441–448.
485 doi:10.1038/s41579-019-0196-3

486 5. Kaplan Y, Reich S, Oster E, Maoz S, Levin-Reisman I, Ronin I, et al. Observation of universal
487 ageing dynamics in antibiotic persistence. Nature. 2021;600: 290–294. doi:10.1038/s41586-
488 021-04114-w

489 6. Lewis K. Persister cells, dormancy and infectious disease. Nature Reviews Microbiology.
490 Nature Publishing Group; 2007. pp. 48–56. doi:10.1038/nrmicro1557

491 7. Pu Y, Li Y, Jin X, Tian T, Ma Q, Zhao Z, et al. ATP-Dependent Dynamic Protein Aggregation
492 Regulates Bacterial Dormancy Depth Critical for Antibiotic Tolerance. Mol Cell. 2019;73: 143-
493 156.e4. doi:10.1016/j.molcel.2018.10.022

494 8. Bamford RA, Smith A, Metz J, Glover G, Titball RW, Pagliara S. Investigating the physiology of
495 viable but non-culturable bacteria by microfluidics and time-lapse microscopy. BMC Biol.
496 2017;15. doi:10.1186/s12915-017-0465-4

497 9. Kim JS, Wood TK. Persistent Persister Misperceptions. Front Microbiol. 2016;7: 2134.
498 doi:10.3389/FMICB.2016.02134

499 10. Goormaghtigh F, Van Melderen L. Single-cell imaging and characterization of Escherichia coli
500 persister cells to ofloxacin in exponential cultures. Sci Adv. 2019;5.
501 doi:10.1126/sciadv.aav9462

502 11. Balaban NQ, Merrin J, Chait R, Kowalik L, Leibler S. Bacterial persistence as a phenotypic
503 switch. Science (80-). 2004;305: 1622–1625. doi:10.1126/science.1099390

504 12. Wakamoto Y, Dhar N, Chait R, Schneider K, Signorino-Gelo F, Leibler S, et al. Dynamic
505 persistence of antibiotic-stressed mycobacteria. Science (80-). 2013;339: 91–95.
506 doi:10.1126/science.1229858

507 13. Roostalu J, Jõers A, Luidalepp H, Kaldalu N, Tenson T. Cell division in Escherichia coli cultures
508 monitored at single cell resolution. BMC Microbiol. 2008;8: 68. doi:10.1186/1471-2180-8-68

14. Orman MA, Brynildsen MP. Dormancy is not necessary or sufficient for bacterial persistence. Antimicrob Agents Chemother. 2013;57: 3230–3239. doi:10.1128/AAC.00243-13

15. Sulaiman JE, Lam H. Evolution of Bacterial Tolerance Under Antibiotic Treatment and Its Implications on the Development of Resistance. Front Microbiol. 2021;12: 617412. doi:10.3389/fmicb.2021.617412

16. Levin-Reisman I, Ronin I, Gefen O, Braniss I, Shoresh N, Balaban NQ. Antibiotic tolerance facilitates the evolution of resistance. Science (80-). 2017;355: 826–830. doi:10.1126/science.aaj2191

17. Levin-Reisman I, Brauner A, Ronin I, Balaban NQ. Epistasis between antibiotic tolerance, persistence, and resistance mutations. Proc Natl Acad Sci U S A. 2019;116: 14734–14739. doi:10.1073/pnas.1906169116

18. Bakkeren E, Huisman JS, Fattinger SA, Hausmann A, Furter M, Egli A, et al. Salmonella persisters promote the spread of antibiotic resistance plasmids in the gut. Nature. 2019;573: 276–280. doi:10.1038/s41586-019-1521-8

19. Barrett TC, Mok WWK, Murawski AM, Brynildsen MP. Enhanced antibiotic resistance development from fluoroquinolone persisters after a single exposure to antibiotic. Nat Commun. 2019;10: 1–11. doi:10.1038/s41467-019-09058-4

20. Liu J, Gefen O, Ronin I, Bar-Meir M, Balaban NQ. Effect of tolerance on the evolution of antibiotic resistance under drug combinations. Science (80-). 2020;367: 200–204. doi:10.1126/science.aay3041

21. El Meouche I, Dunlop MJ. Heterogeneity in efflux pump expression predisposes antibiotic-resistant cells to mutation. Science (80-). 2018. doi:10.1126/science.aar7981

22. Wang P, Robert L, Pelletier J, Dang WL, Taddei F, Wright A, et al. Robust growth of Escherichia coli. Curr Biol. 2010;20: 1099–103. doi:10.1016/j.cub.2010.04.045

23. Jouvet L, Rodríguez-Rojas A, Steiner UK. Demographic variability and heterogeneity among individuals within and among clonal bacteria strains. Oikos. 2018;127: 728–737. doi:10.1111/oik.04292

24. Steiner UK, Lenart A, Ni M, Chen P, Song X, Taddei F, et al. Two stochastic processes shape diverse senescence patterns in a single-cell organism. Evolution (N Y). 2019;73: 847–857. doi:10.1111/evo.13708

25. Knudsen GM, Fromberg A, Ng Y, Gram L. Sublethal concentrations of antibiotics cause shift to anaerobic metabolism in Listeria monocytogenes and induce phenotypes linked to antibiotic tolerance. Front Microbiol. 2016;7: 1091. doi:10.3389/FMICB.2016.01091/BIBTEX

26. Melnyk AH, Wong A, Kassen R. The fitness costs of antibiotic resistance mutations. Evol Appl. 2015;8: 273–283. doi:10.1111/eva.12196

27. Rossi NA, El Meouche I, Dunlop MJ. Forecasting cell fate during antibiotic exposure using stochastic gene expression. Commun Biol. 2019;2: 1–7. doi:10.1038/s42003-019-0509-0

28. Dörr T, Lewis K, Vulić M. SOS response induces persistence to fluoroquinolones in Escherichia coli. PLoS Genet. 2009;5: e1000760. doi:10.1371/journal.pgen.1000760

29. Rodríguez-Rojas A, Baeder DY, Johnston P, Regoes RR, Rolff J. Bacteria primed by antimicrobial peptides develop tolerance and persist. PLOS Pathogens. PLoS Biol; 2021. p. e1009443. doi:10.1371/journal.ppat.1009443

551 30. Windels EM, Van den Bergh B, Michiels J. Bacteria under antibiotic attack: Different strategies
552 for evolutionary adaptation. Silverman N, editor. PLOS Pathog. 2020;16: e1008431.
553 doi:10.1371/journal.ppat.1008431

554 31. Balaban NQ, Liu J. Evolution under antibiotic treatments: Interplay between antibiotic
555 persistence, tolerance, and resistance. Persister Cells and Infectious Disease. Springer
556 International Publishing; 2019. pp. 1–17. doi:10.1007/978-3-030-25241-0_1

557 32. Fridman O, Goldberg A, Ronin I, Shoresh N, Balaban NQ. Optimization of lag time underlies
558 antibiotic tolerance in evolved bacterial populations. Nature. 2014;513: 418–421.
559 doi:10.1038/nature13469

560 33. Van Den Bergh B, Michiels JE, Wenseleers T, Windels EM, Boer P Vanden, Kestemont D, et al.
561 Frequency of antibiotic application drives rapid evolutionary adaptation of Escherichia coli
562 persistence. Nat Microbiol. 2016;1: 1–7. doi:10.1038/nmicrobiol.2016.20

563 34. Sulaiman JE, Lam H. Proteomic Investigation of Tolerant Escherichia coli Populations from
564 Cyclic Antibiotic Treatment. J Proteome Res. 2020;19: 900–913.
565 doi:10.1021/acs.jproteome.9b00687

566 35. Lee JH, Lee J. Indole as an intercellular signal in microbial communities. FEMS Microbiology
567 Reviews. Blackwell Publishing Ltd; 2010. pp. 426–444. doi:10.1111/j.1574-6976.2009.00204.x

568 36. Diez S, Ryu J, Caban K, Gonzalez RL, Dworkin J. The alarmones (p)ppGpp directly regulate
569 translation initiation during entry into quiescence. Proc Natl Acad Sci U S A. 2020;117: 15565–
570 15572. doi:10.1073/pnas.1920013117

571 37. Vega NM, Allison KR, Khalil AS, Collins JJ. Signaling-mediated bacterial persister formation.
572 Nat Chem Biol. 2012;8: 431–433. doi:10.1038/nchembio.915

573 38. Maisonneuve E, Gerdes K. Molecular mechanisms underlying bacterial persisters. Cell. Cell
574 Press; 2014. pp. 539–548. doi:10.1016/j.cell.2014.02.050

575 39. Van Acker H, Van Dijck P, Coenye T. Molecular mechanisms of antimicrobial tolerance and
576 resistance in bacterial and fungal biofilms. Trends in Microbiology. Elsevier Ltd; 2014. pp.
577 326–333. doi:10.1016/j.tim.2014.02.001

578 40. Olsen I. Biofilm-specific antibiotic tolerance and resistance. European Journal of Clinical
579 Microbiology and Infectious Diseases. Springer Verlag; 2015. pp. 877–886.
580 doi:10.1007/s10096-015-2323-z

581 41. Harms A, Maisonneuve E, Gerdes K. Mechanisms of bacterial persistence during stress and
582 antibiotic exposure. Science (80-). 2016;354. doi:10.1126/science.aaf4268

583 42. Michiels JE, Van den Bergh B, Verstraeten N, Michiels J. Molecular mechanisms and clinical
584 implications of bacterial persistence. Drug Resist Updat. 2016;29: 76–89.
585 doi:10.1016/j.drup.2016.10.002

586 43. Page R, Peti W. Toxin-antitoxin systems in bacterial growth arrest and persistence. Nat Chem
587 Biol. 2016;12: 208–214. doi:10.1038/nchembio.2044

588 44. Wilmaerts D, Windels EM, Verstraeten N, Michiels J. General Mechanisms Leading to
589 Persister Formation and Awakening. Trends in Genetics. Elsevier Ltd; 2019. pp. 401–411.
590 doi:10.1016/j.tig.2019.03.007

591 45. Harms A, Fino C, Sørensen MA, Semsey S, Gerdes K. Prophages and growth dynamics
592 confound experimental results with antibiotic-tolerant persister cells. MBio. 2017;8.
593 doi:10.1128/mBio.01964-17

46. Shah D, Zhang Z, Khodursky A, Kaldalu N, Kurg K, Lewis K. Persisters: A distinct physiological state of E. coli. BMC Microbiol. 2006;6: 1–9. doi:10.1186/1471-2180-6-53

47. Khare A, Tavazoie S. Extreme Antibiotic Persistence via Heterogeneity-Generating Mutations Targeting Translation. mSystems. 2020;5. doi:10.1128/msystems.00847-19

48. Zahir T, Wilmaerts D, Franke S, Weytjens B, Camacho R, Marchal K, et al. Image-Based Dynamic Phenotyping Reveals Genetic Determinants of Filamentation-Mediated β-Lactam Tolerance. Front Microbiol. 2020;11: 374. doi:10.3389/fmicb.2020.00374

49. R Core Team RA language and environment for statistical computing. R: A language and environment for statistical computing. Team RDC, editor. R Foundation for Statistical Computing. Vienna, Austria: R Foundation for Statistical Computing; 2016. p. 409. doi:10.1007/978-3-540-74686-7

50. Burnham K, Anderson DR. Model selection and multimodel inference : a practical information-theoretic approach. Second. New York: Springer; 1998.